Cell Reports Medicine, Volume *5*

Supplemental information

Bifidobacteria with indole-3-lactic acid-producing capacity exhibit psychobiotic potential via reducing neuroinflammation

Xin Qian, Qing Li, Huiyue Zhu, Ying Chen, Guopeng Lin, Hao Zhang, Wei Chen, Gang Wang, and Peijun Tian

Bifidobacteria with Indole-3-Lactic Acid Producing Capacity Exhibit Psychobiotic Potential via Reducing Neuroinflammation

Xin Qian[1, 2], Qing Li[1, 2], Huiyue Zhu[1, 2], Ying Chen[1, 2], Guopeng Lin[1, 2], Hao Zhang[1, 2, 3, 4], Wei Chen[1, 2, 3], Gang Wang[1, 2], Peijun Tian[1, 2, 5, *]

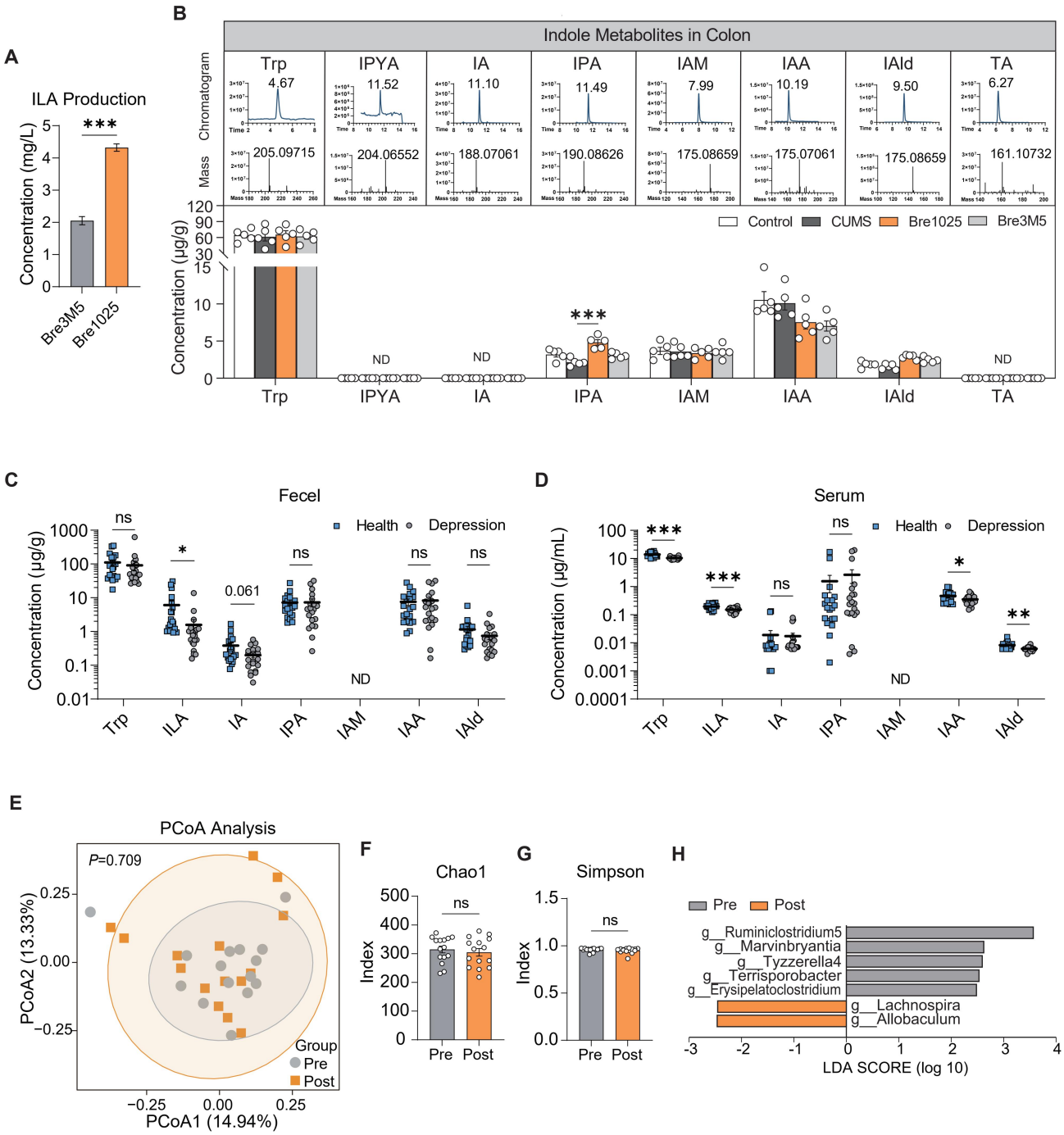

Figure S1. Regulation of indole derivatives metabolism by *B. breve* in CUMS model mice and human subjects, related to Figure 1 and 2.

(A) ILA production by Bre3M5 or Bre1025 in mMRS. **(B)** Concentrations of tryptophan (Trp) and indole derivatives in mouse colon content. Chromatogram/Mass: chromatogram/mass spectra of the corresponding indole derivative, respectively. IPYA: Indole-3-pyruvate; IA: Indole acrylic acid; IPA: Indole-3-propionic acid; IAM: Indole-3-acetamide; IAA: Indole-3-acetic acid; IAld: Indole-3-aldehyde; TA: tryptamine. ND: not detected. **(C-D)** Concentrations of indole derivatives in feces (C) and serum (D) of patients with depressive disorder. **(E)** β-diversity analysis of gut microbiota in healthy human subjects pre and post Bre1025 intake. Principal coordinates analysis (PCoA) based on Bray-Curtis dissimilarity. **(F-G)** α-diversity analysis, including Chao1 index (F) and Simpson index (G). **(H)** Linear discriminant analysis effect size (LDA) analysis. *p < 0.05, **p < 0.01, ***p < 0.001,determined by unpaired two-tailed Student's t-test in (A), one-way ANOVA followed by Sidak post hoc test in (B) and paired two-tailed Student's t-test in (F and G).

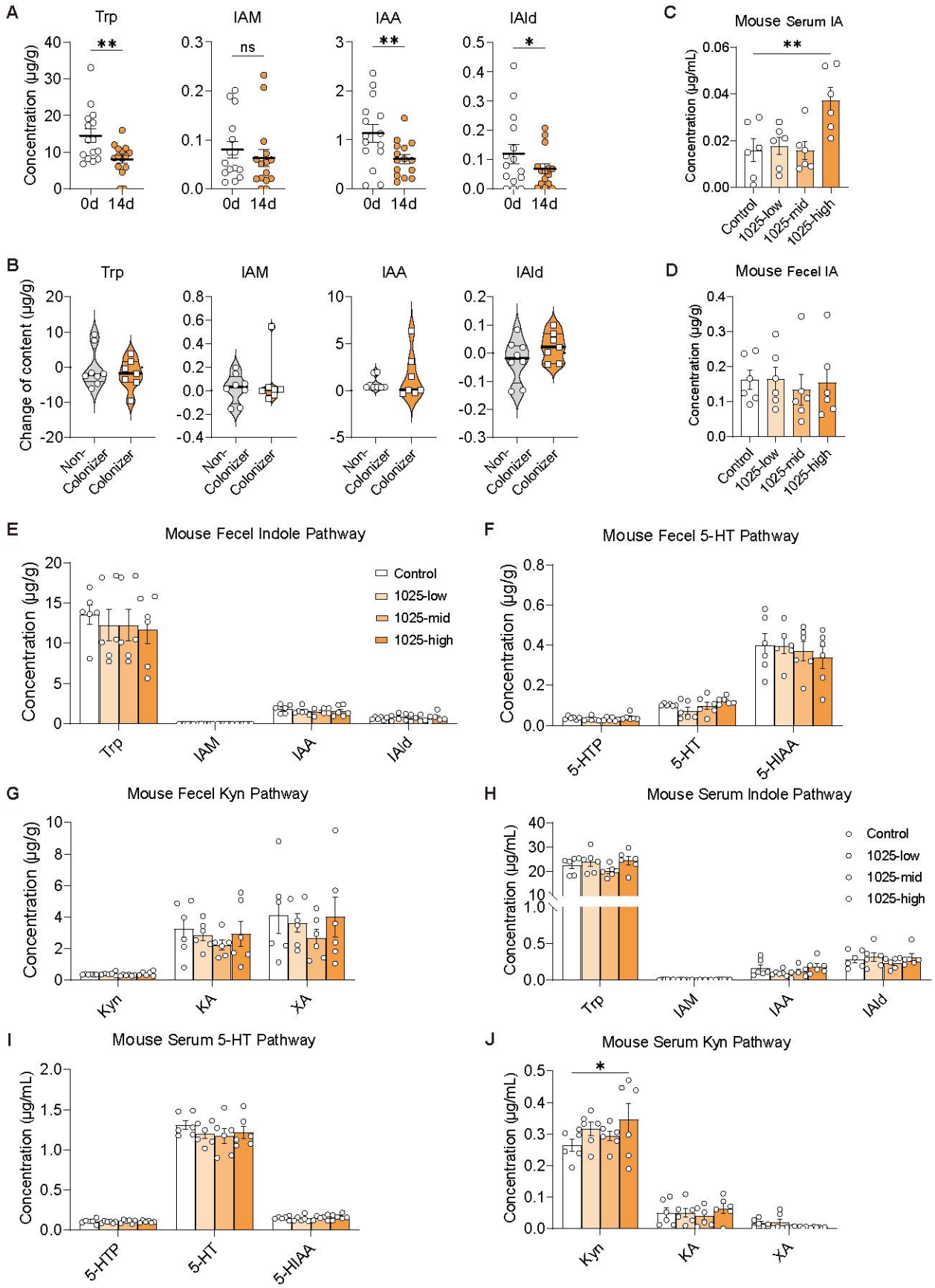

Figure S2. Effect of Bre1025 on intestinal indole derivative content in healthy volunteers, related to Figure 2.
(A) Effect of continuous ingestion of Bre1025 on intestinal indole derivative content. **(B)** Effect of Bre1025 on intestinal indole derivative content after washout. **(C and D)** Concentrations of Indole acrylic acid (IA) in mouse serum (B) and feces (D). **(E-G)** Metabolite content of Trp-Indole pathway (E), Trp-5-HT pathway (F) and Trp-Kyn pathway (G) in mouse feces. 5-HT: 5-hydroxytryptamine, 5-HTP: 5-hydroxytryptophan; 5-HIAA: 5-hydroxyindoleacetic acid; Kyn: kynurenine; KA: kynurenic acid; XA: xanthurenic acid. **(H-J)** Metabolite content of Trp-Indole pathway (E), Trp-5-HT pathway (F) and Trp-Kyn pathway (G) in mouse serum. *$p < 0.05$, **$p < 0.01$, determined by two-tailed paired Student's t-test in (A and B) and one-way ANOVA followed by Sidak post hoc test in (C-J).

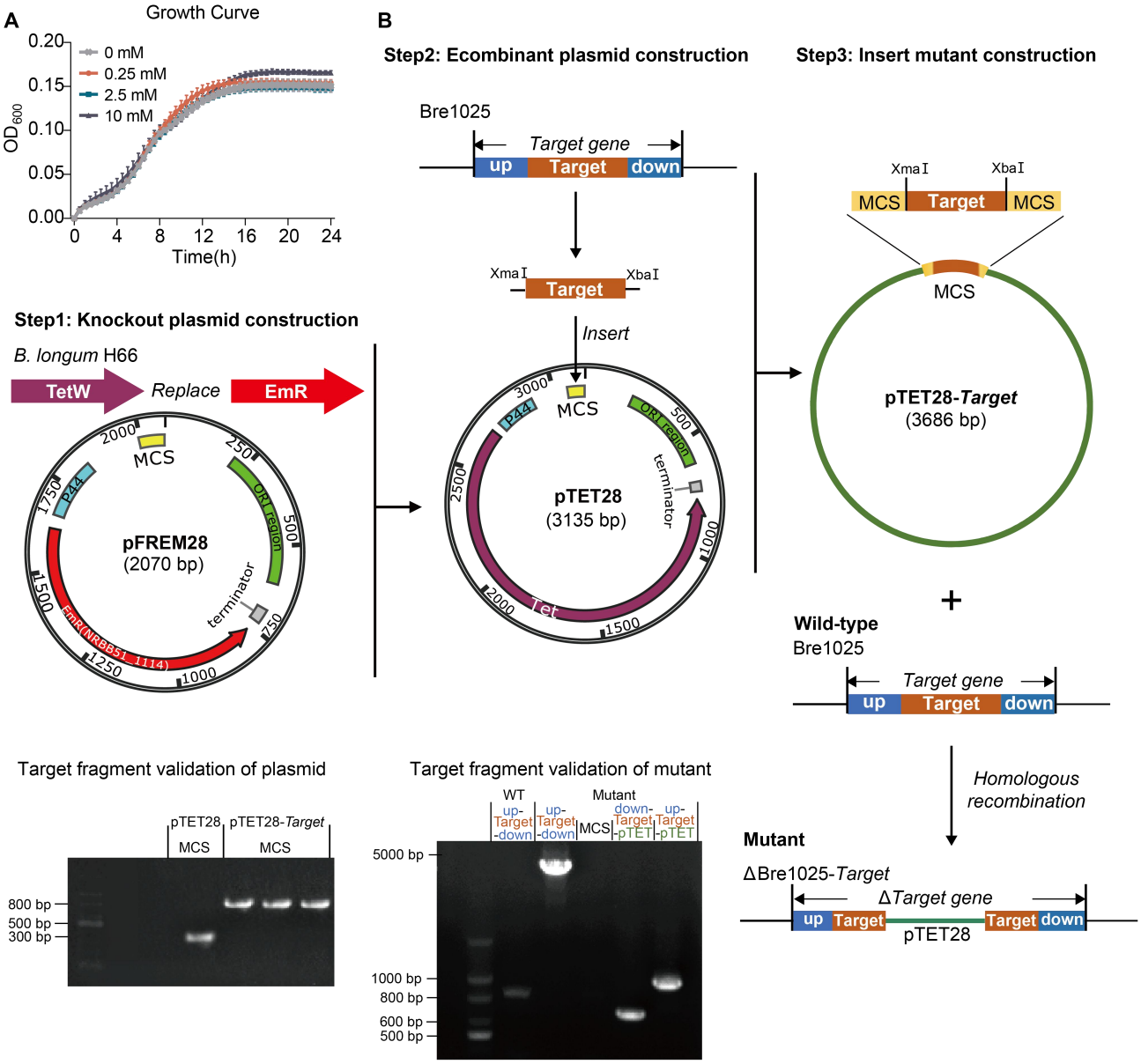

Figure S3. Tryptophan metabolism of Bre1025 and construction of tryptophan metabolic-related gene mutants, related to Figure 3 and STAR Methods.

(A) *In vitro* growth of Bre1025 at different tryptophan substrate concentrations. **(B)** Construction of the Bre1025 gene mutant strain. pTET28-*Target*: recombinant plasmid of pTET28 and Target gene fragment; WT: wild-type; ΔBre1025-*Target*: mutant strain of the Bre1025 target gene; MCS: multiple cloning site; up-Target-down: fragment from the up region to the down region of the target gene in the strain; down/up-Target-pTET: the cross junction site fragment from the down/up region to the pTET28 region of the target gene in the mutant strain.

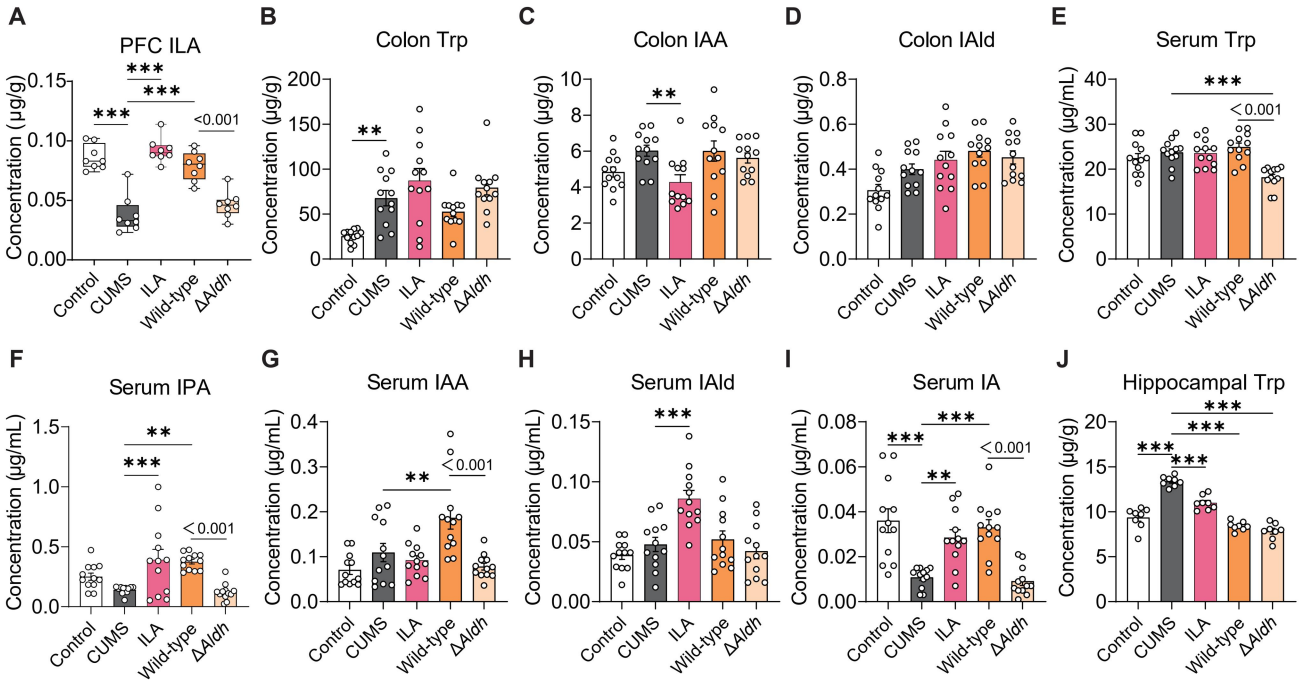

Figure S4. Effect of *Aldh* gene on the regulation of indole metabolism by Bre1025 in CUMS model mice, related to Figure 4.

(A-G) Concentrations of Trp and indole derivatives in mouse colon content, serum, prefrontal cortex (PFC) and hippocampus. **p < 0.01, ***p < 0.001, determined by one-way ANOVA followed by Sidak post hoc test.

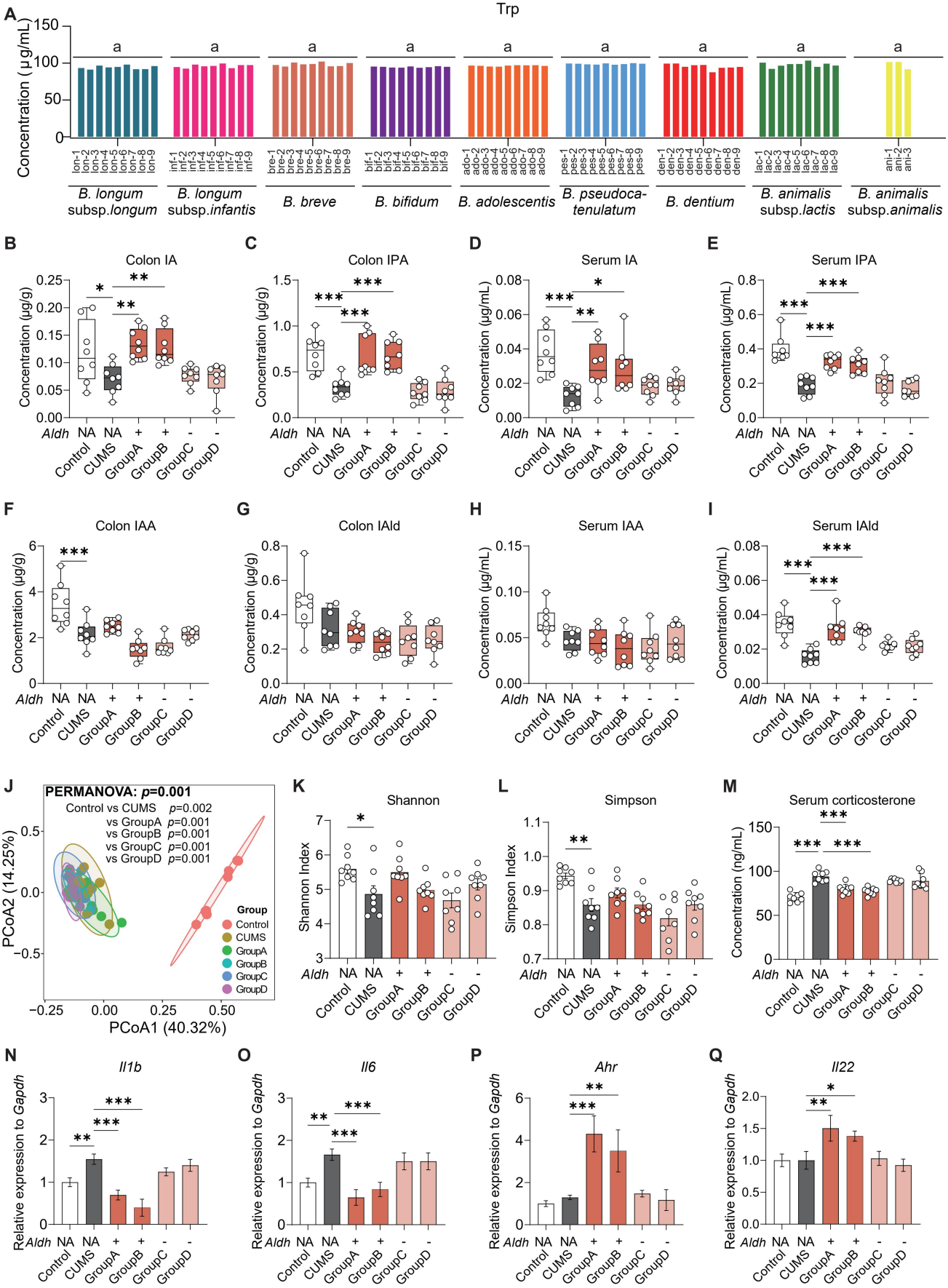

Figure S5. Regulation of Trp-indole metabolism by bifidobacteria, related to Figure 5.

(A) Tryptophan depletion *in vitro* of diverse *Bifidobacterium* species. **(B-I)** Concentrations of indole derivatives in mouse colon content and serum. **(J)** Principal component analysis of gut microbiota in mice after intervention with different bifidobacteria. **(K and L)** Shannon and Simpson indexes of α-diversity of gut microbiota in mice after intervention with different bifidobacteria. **(M)** Serum corticosterone concentrations in mice after intervention with different bifidobacteria. **(N-Q)** Gene expression of interleukin-1β (IL-1β, N), IL-6 (O), AhR (P) and IL-22 (Q) in mouse hippocampus. *p < 0.05, **p < 0.01, ***p < 0.001, determined by one-way ANOVA followed by Sidak post hoc test.

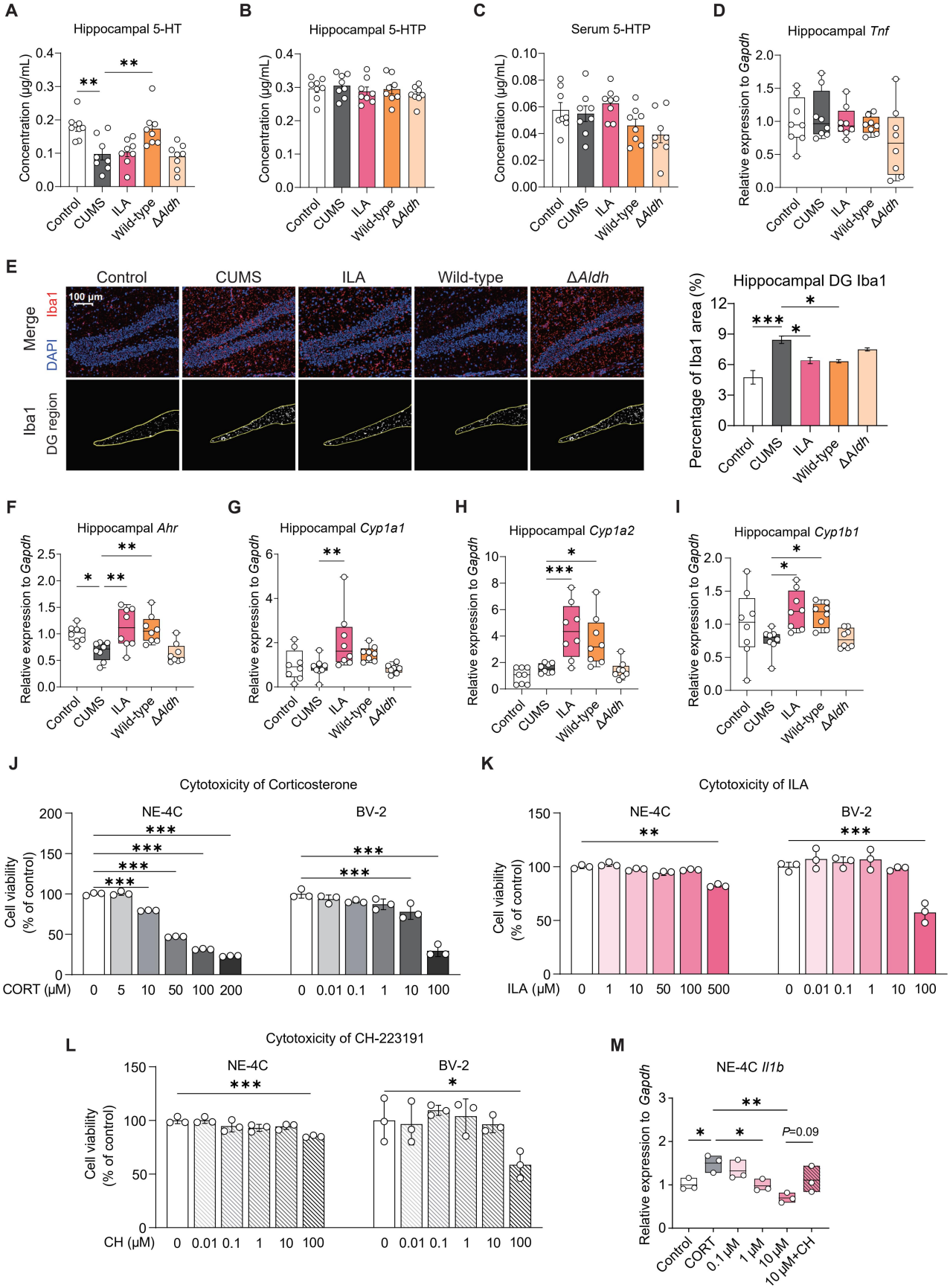

Figure S6. Bifidobacteria alleviates neuroinflammation by producing ILA, related to Figure 6.

(A) Concentrations of 5-HT in mouse hippocampus. **(B and C)** Concentrations of 5-HTP in mouse hippocampus (B) and serum (C). **(D)** Expression of tumor necrosis factor-α (*Tnf*) in the hippocampus. **(E)** Immunofluorescence detection of Iba1 in mouse brain. DG: Dentate gyrus of hippocampus. **(F-I)** Expression of AhR signaling in the hippocampus of mice. *Ahr* (F), *Cyp1a1* (G), *Cyp1a2* (H) and *Cyp1b1* (I) gene expression. **(J-K)** Cytotoxicity of corticosterone (J), ILA (K) and CH-223191 (L) on NE-4C and BV-2 activity. **(M)** Gene expression of IL-1β in the NE-4C cell. *p < 0.05, **p < 0.01, ***p < 0.001, determined by one-way ANOVA followed by Sidak post hoc test.